Released on 30/11/2016 in Luxembourg

EXPERIMENTAL TESTING OF THE "ACTIVMOTION" PLATE

By

Dr. Arnaud Diffo Kaze

Contributors :

Pr. Stefan Maas, University of Luxembourg

Pr. Dietrich Pape, University Clinic of Saarland

BIOMECHANICAL COMPARATIVE STUDY OF 6 DIFFERENTS OSTEOSYNTHESIS SYSTEMS FOR VALGISATION HIGH TIBIAL OSTEOTOMY: EXPERIMENTAL TESTS

Content

1. Introduction

The aim of the present study was to test and to compare mechanical static and fatigue strength of the size 2 osteotomy plate “Activmotion” (**Figure 1**) of the company Newclip Technics (Haute-Goulaine, France) with five other implants for the treatment of medial knee joint osteoarthritis using a testing procedure that was already previously defined, used and published (Maas, Diffo Kaze, Dueck, & Pape, 2013; Diffo Kaze, et al., 2015; Diffo Kaze A. , 2016). These other comparative implants are the Contour Lock plate, the iBalance implant, the PEEKPower plate of Arthrex (Munich, Germany), the TomoFix small stature (TomoFix sm) and the TomoFix standard (TomoFix std) plates of Synthes Gmbh (Oberdorf, Switzerland) (**Figure 2**).

Figure 1: Size 2 Activmotion plate

The tested specimens are plate and artificial bone constructs, subjected to static and cyclic testing to failure as described in (Maas, Diffo Kaze, Dueck, & Pape, 2013; Diffo Kaze, et al., 2015; Diffo Kaze A. , 2016).

Figure 2: (A) Contour Lock HTO plate, (B) TomoFix small stature plate (TomoFix sm) , (C) TomoFix Standard plate (TomoFix std), (D) PEEKPower plate and (E) iBalance implant.

2. Methods

Six large-size fourth generation composite analogue tibia bone models (Sawbones, Pacific Research Laboratories, Inc., Vashon, WA) were used for the tests. Opening wedge proximal medial osteotomies were performed on each of the composite bones in the same way by an experienced surgeon, according to standard techniques of the plate. The same standardized procedure as by the last performed osteotomy tests (Maas, Diffo Kaze, Dueck, & Pape, 2013; Diffo Kaze, et al., 2015; Diffo Kaze A. , 2016) has been used to prepare the specimens.

For the static tests, the specimens were subjected to a quasi-static compression displacement-controlled single loading to failure at a speed of 0.1 mm/s, while the dynamic tests, according to **Figure 3**, consisted in load-controlled cyclical fatigue testing, with stepwise compression sinusoidal (frequency = 5Hz) loading where the force amplitude of each step was kept constant with feed-back control of the force signal within the hydraulic machine. The lower compressive force limit of each load step was kept constant at 160 N. Starting from 800 N for the first step the upper compressive force limit was increased stepwise by 160 N after N=20000 cycles if no failure occurred. This testing procedure is similar to the standardized testing protocol for hip joints (ISO 7206-4, 1989; ISO 7206-6, 1992; ISO 7206-8, 1995).

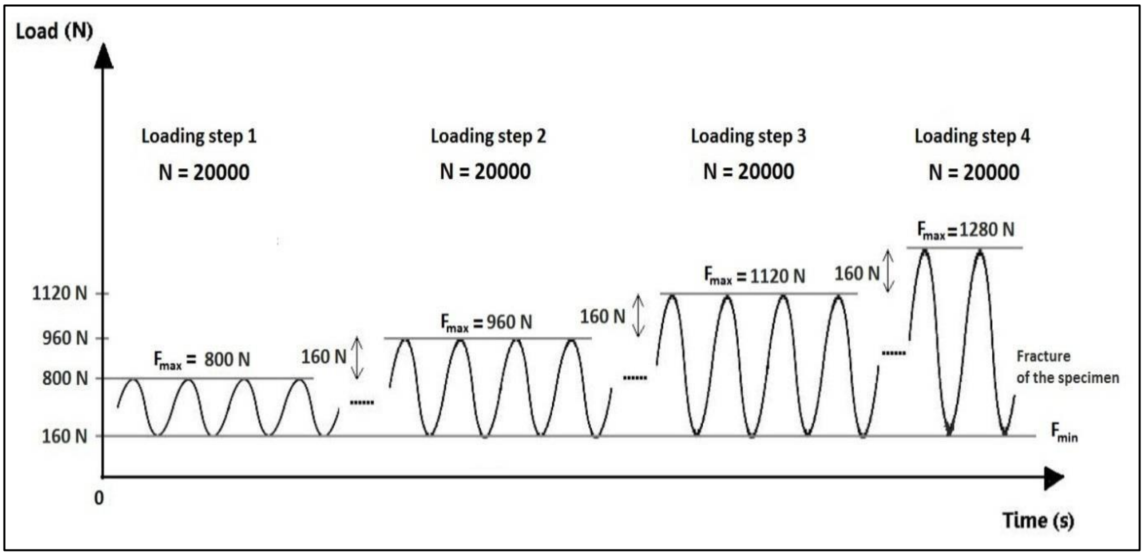

Figure 3: Scheme of the applied vertical sinusoidal force loading (load-controlled) After N=20.000 cycles the upper force is increased stepwise by 160 N until failure. The loading frequency was constant and set to 5 Hz.

A total of 6 specimens were used as indicated in **Table 1**.

Performed test	Specimens
Static: Single loading to failure test	Activmotion 1
	Activmotion 2
Dynamic: cyclical fatigue failure test	Activmotion 3
	Activmotion 4
	Activmotion 5
	Activmotion 5

Table 1: Specimen subdivision depending on the performed test

Purely vertical loading was applied to the tibia head of the specimens (**Figure 4-A**) through a freely movable support allowing any horizontal motion in the transversal plane using three freely rolling metal balls (**Figure 4-B**). The **Figure 4-C** shows the positions of the displacements sensors used to capture the deformation of the specimens. The displacement in the frontal plane on the medial side of the tibia head was measured by the medial sensor MS. A second sensor LS at the lateral side measured the lateral displacement. Three displacement sensors DX and DY1 and DY2 were attached on the easily sliding support in order to measure the horizontal displacements of the tibia head in two perpendicular directions. A fifth displacement sensor VS embedded in the INSTRON machine measured the vertical displacement of piston.

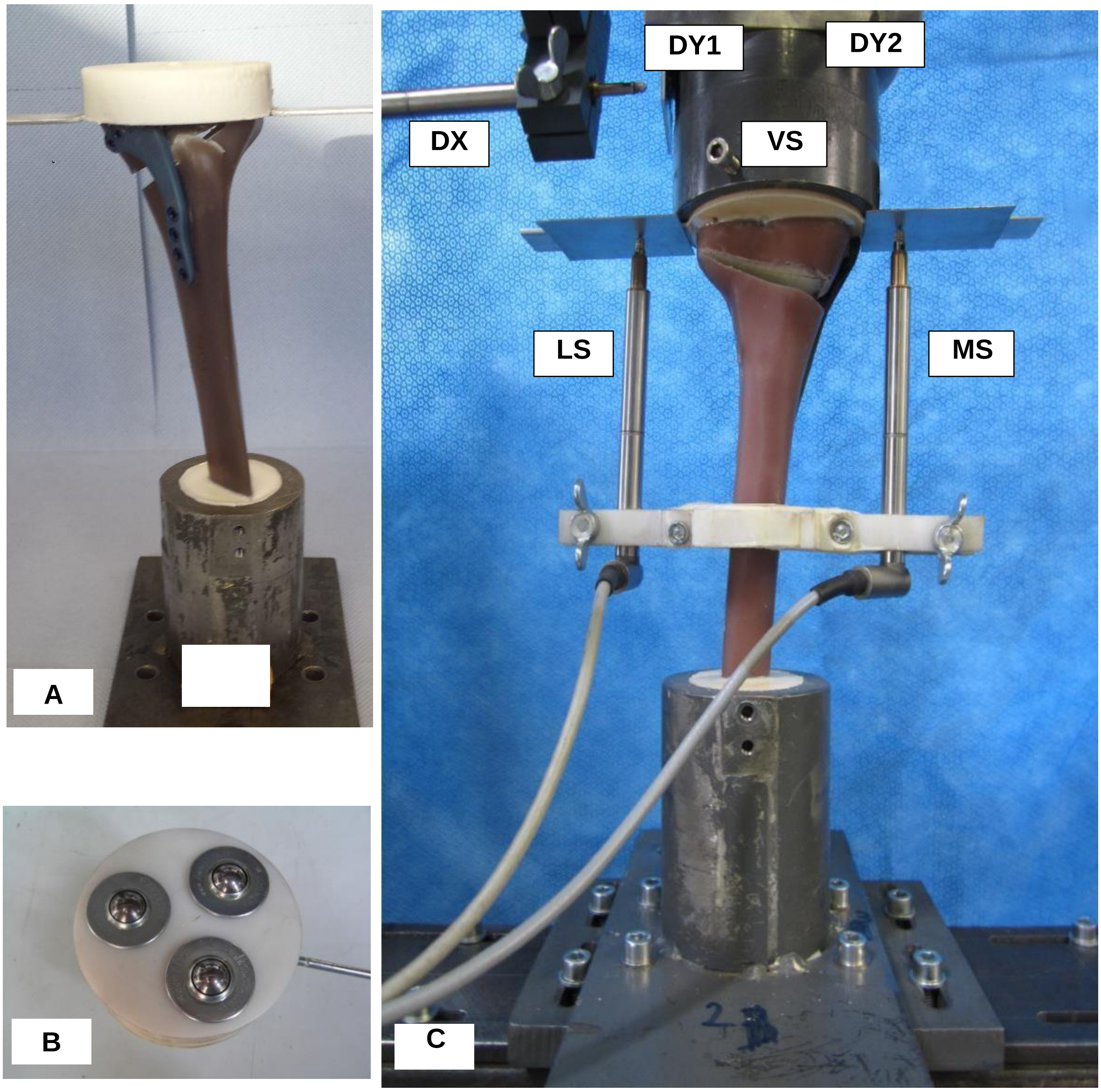

Figure 4: (A) Specimen before mounting to hydraulic press. (B) Low friction sliding support to apply purely vertical forces. (C) Specimen under test: The lateral and the medial sensor (LS and MS) register the relative lateral and medial vertical displacements from the tibial head, while VS measured its vertical displacement. The sensors DX, DY1 and DY2 register the horizontal displacements of the tibial head; along the transverse axis for the first and the sagittal axis for the latter.

The **Table 2** summarizes the failure criteria that have been considered within this study. This criteria were already used by Pape et al (Pape, D.; Lorbach, O.; Schmitz, C.; Busch, L. C.; Van Giffen, N.; Seil, R.; Kohn, D. M., 2010). The failure type 3 allows quantifying the wobble degree or the stability of the sample during the cyclic testing (Maas, Diffo Kaze, Dueck, & Pape, 2013; Diffo Kaze, et al., 2015; Diffo Kaze A. , 2016).

Failure type	Criteria
1	Medial or lateral displacements of the tibial head in relation to the tibial shaft of more than 2 mm. This criterion can only be checked in the unloaded condition. .
2	Visible collapse of lateral cortex. Small hairline cracks are not considered as failure.
3	Maximal displacement range of more than 0.5 mm within one hysteresis loop in the case of cyclic testing only.
4	Cracks of the screws of more than 1 mm

Table 2: Used failure types and their defining criteria (Maas, Diffo Kaze, Dueck, & Pape, 2013; Diffo Kaze, et al., 2015; Diffo Kaze A. , 2016).

3. Static loading to failure

The following pictures (**Figure 5** and **Figure 6**) show the characteristic curves (force versus registered displacements) for the specimens Activmotion 1 and 2 obtained from the static tests.

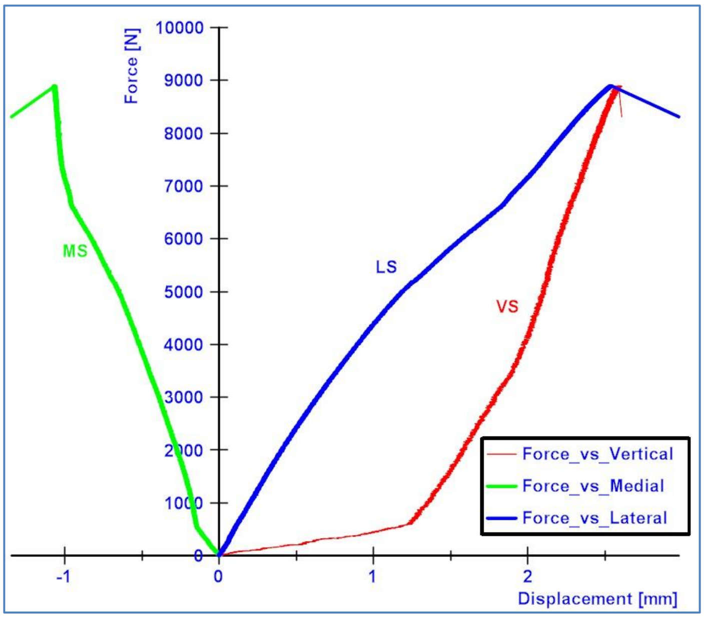

Figure 5: First static test results (Activmotion 1)

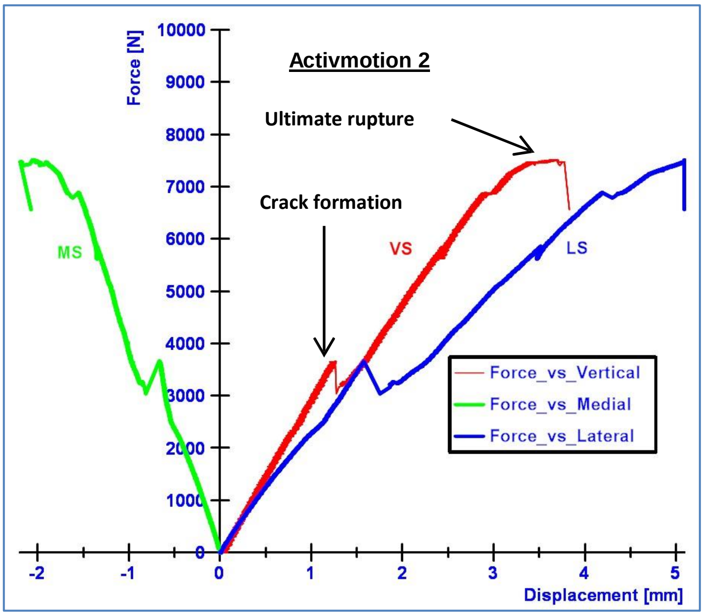

Figure 6: Second static test results (Activmotion 2)

The specimens Activmotion 1 and 2 failed by fracture of the contralateral cortical bone (**Figure 7** and **Figure 8**). The ultimate fracture in the case of Activmotion 2 was preceded by cracks formation (**Figure 6**).

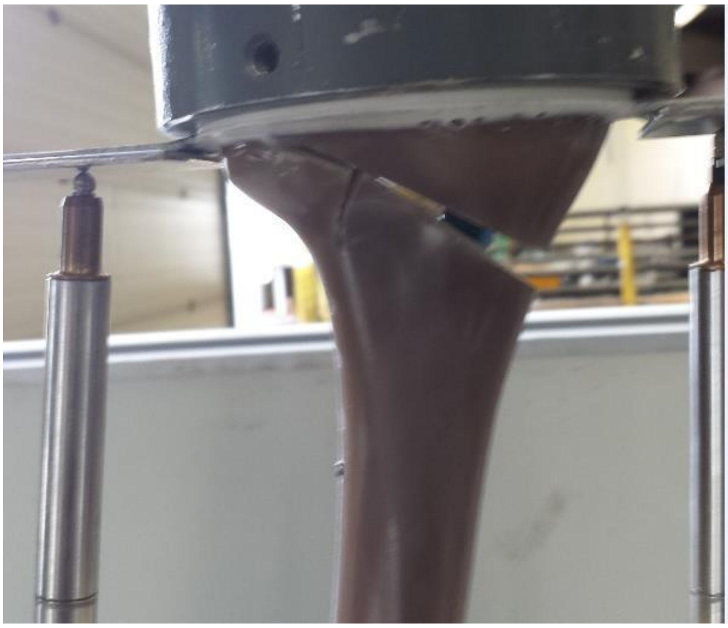

Figure 7: Fracture of the lateral cortical (Activmotion 1)

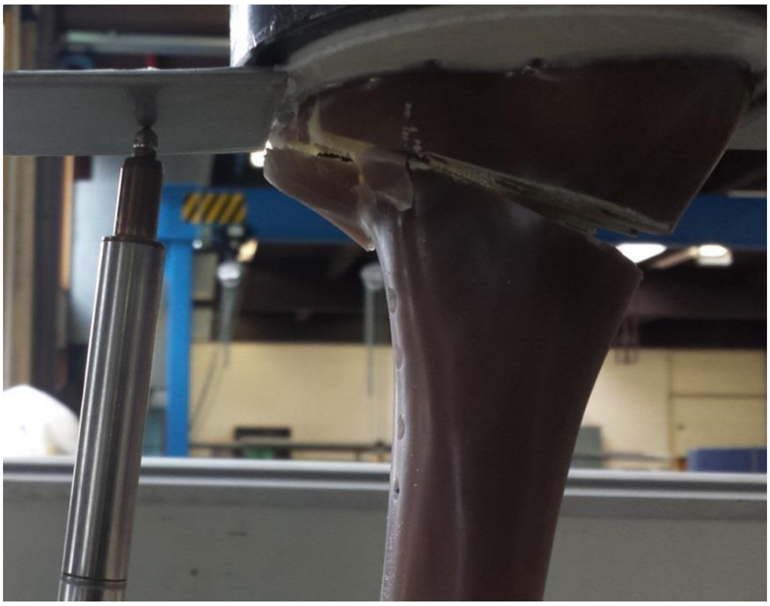

Figure 8: Fracture of the lateral cortical (Activmotion 2)

No defects of the plates or screws were observed.

The **Table 3** summarizes the crack loads at which cracks eventually occurs prior to the ultimate ruptures of the specimen, the ultimate loads and the corresponding displacements. The ultimate load was 8900 N that corresponded to the ultimate medial and lateral displacements 1.3 mm and 2.5 mm respectively. For the Activmotion 2 the crack load was 3700 N, followed by an ultimate load of 7500 N, which corresponded to an ultimate medial displacement of 2.1 mm and lateral displacement of 5.1 mm.

Specimen	Crack load / Ultimate load [N]			Medial displ. at crack- & ultimate load [mm]			Lateral displ. at crack- & ultimate load [mm]		
Activmotion 1	-/8900	**Mean**	**SD±**	- / 1.3	**Mean**	**SD±**	- / 2.5	**Mean**	**SD±**
Activmotion 2	3700/7500	**- /8200**	**- /700**	0.7 / 2.1	**- /1.7**	**- /0.4**	1.6 / 5.1	**- / 3.8**	**- / 1.3**

Table 3: Static tests summary: displacements (displ.) and their corresponding damage loads

By considering the direction of the applied load as positive, that means the descending vertical direction, hence the medial displacements (MS) are negative and the lateral displacements are positive (**Figure 9**). The lateral displacement are greater than the medial displacements, hence the tibial plateau of the specimens, Activmotion 1 and 2, rotated during the static loading.

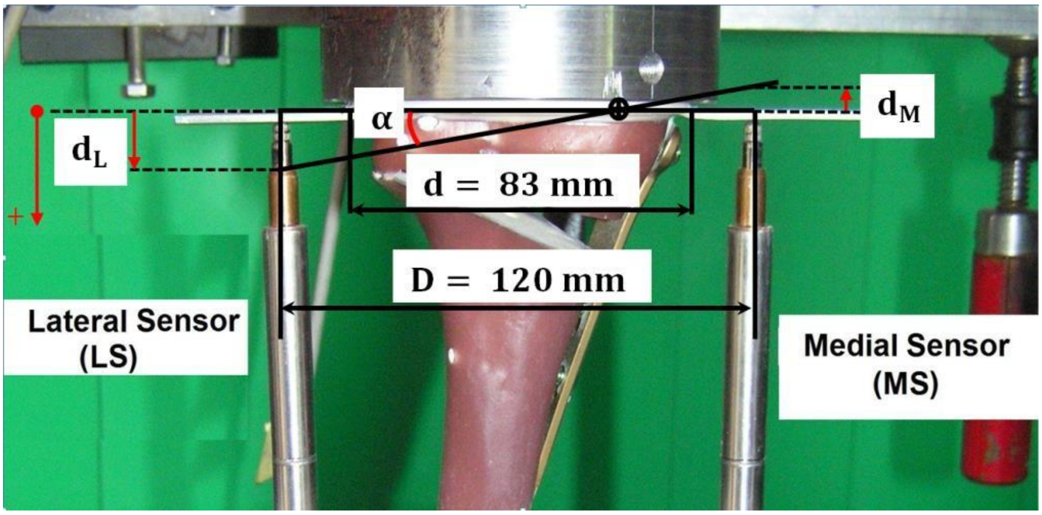

Figure 9: Definition of the positive displacement direction. The lateral displacement d_L was positive and of greater magnitude than the medial displacement d_M that was count negative. The angle α represents the valgus-malrotation of the tibia head and is calculated by mean of the difference $d_L - d_M$

4. Fatigue loading to failure

The fracture of the specimens subjected to cyclical tests occurred in the region of the contralateral cortex (**Figure 10**), as for the static tests. If cracks occurred prior to the final failure of the specimens, they were generally not observable, except in the case of the specimen Activmotion 4 (**Figure 11**), where the crack formation was visible. The plates and screws remained undamaged during the cyclical testing.

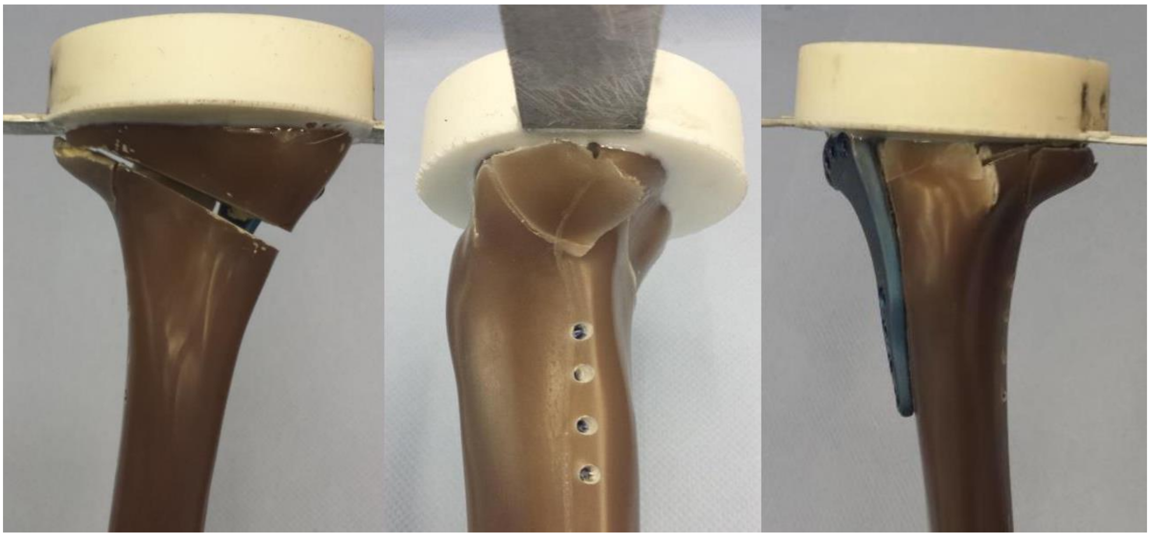

Figure 10: Fracture of the contralateral cortical bone

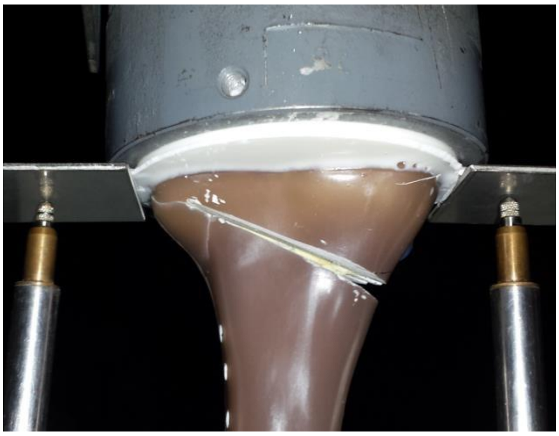

Figure 11: Observable cracking of the contralateral cortex during the cyclical test (Activmotion 4)

During the cyclic loading the tibia head of all the specimens generally rotated counterclockwise, such that the displacement registered by the medial sensor have been counted negative, because the descending vertical direction has been considered to be positive (**Figure 9**).

4.1. Time histories of the applied forces and the vertical, lateral and medial displacements of the specimens

The following plots (from **Figure 12** to **Figure 15**) show the time evolution of the applied force and the registered vertical, the medial and the lateral displacements for all the specimen that have been subjected to the load controlled fatigue tests.

The fracture of the contralateral cortex of the specimen Activmotion 3 occurred at the beginning of load step 10 (LS 10) (**Figure 12**). For the specimen Activmotion 4, the fracture of the contralateral cortex occurred by the end of load step 10. It was preceded by an observable crack formation, which started during the load step 9 and grew to complete fracture at the end of LS 10 (**Figure 13**).

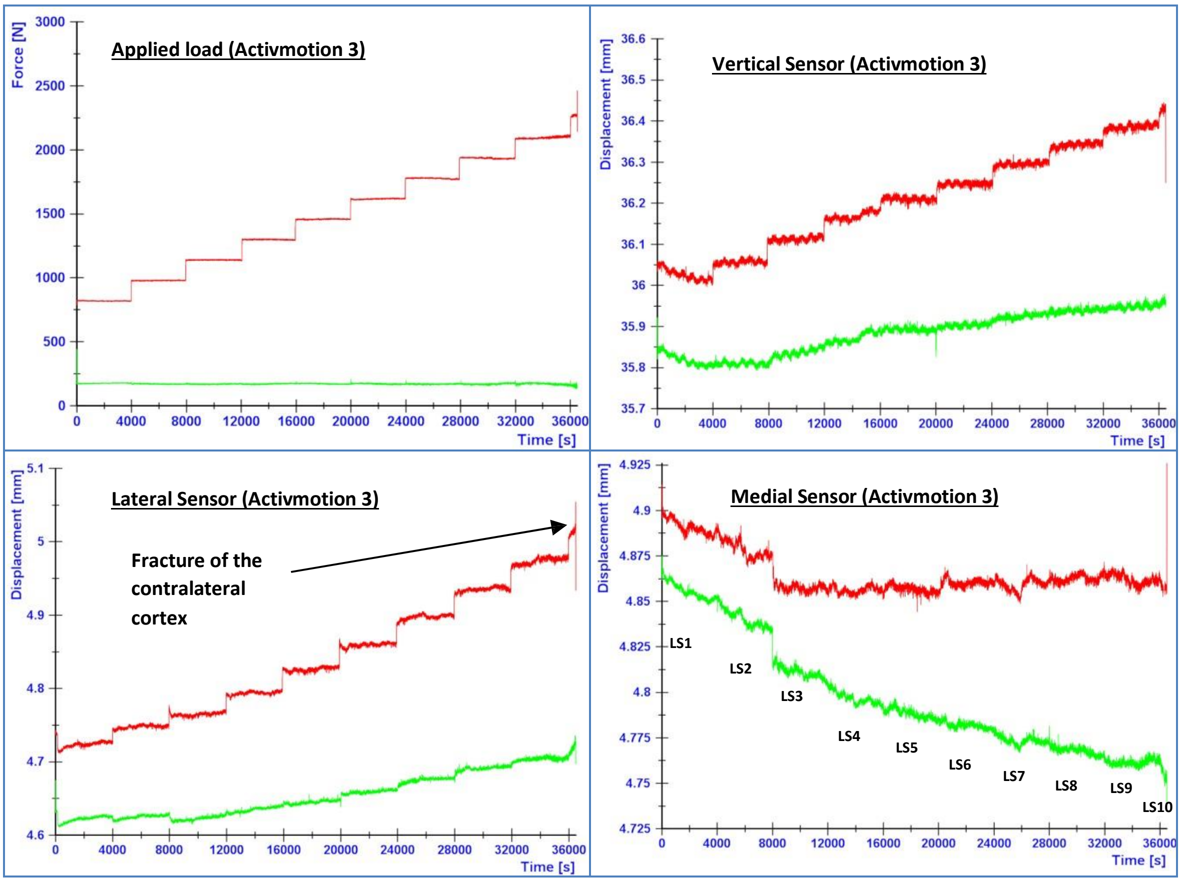

Figure 12: Activmotion 3: Time histories of the applied load, the vertical, the medial and lateral displacements

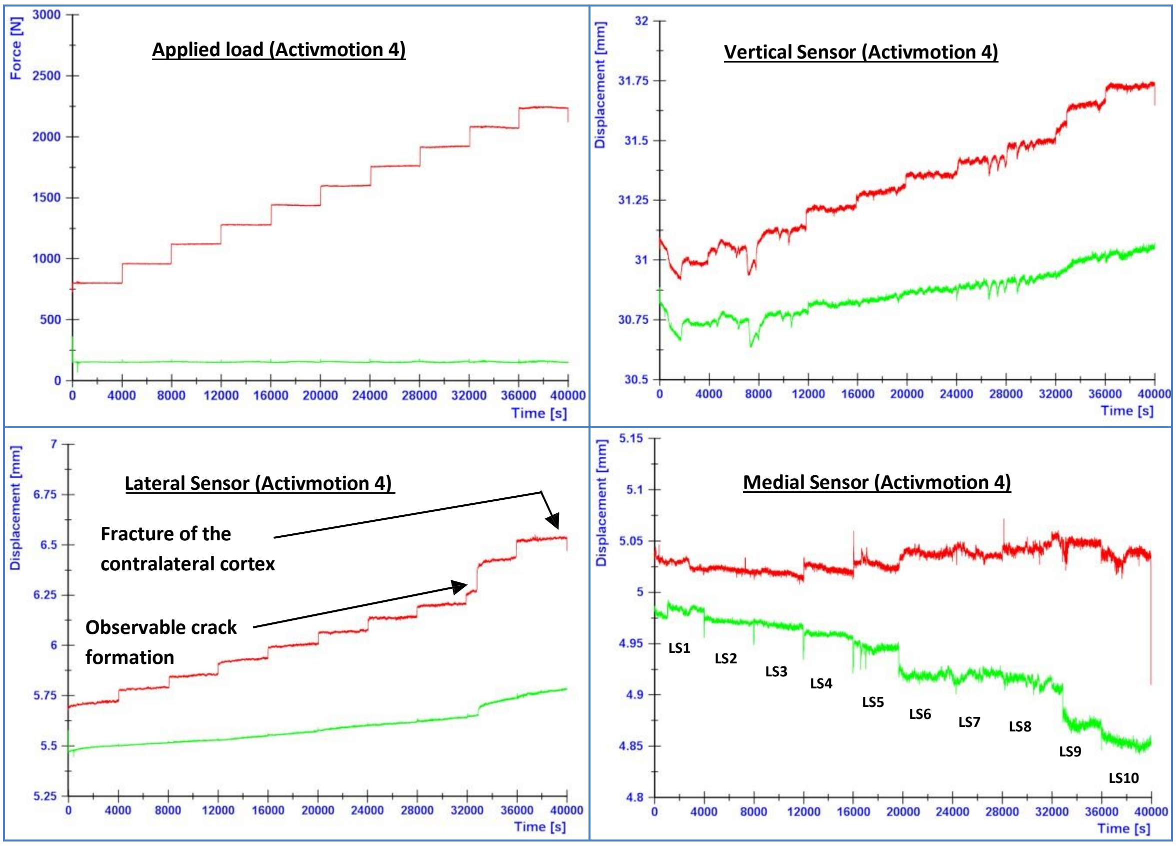

Figure 13: Activmotion 4: Time histories of the applied load, the vertical, the medial and lateral displacements

In the cases of specimens Activmotion 5 and 6, an abrupt fracture of the contralateral cortex occurred during the load step 6 and was not preceded by observable cracking (**Figure 14** and **Figure 15**)

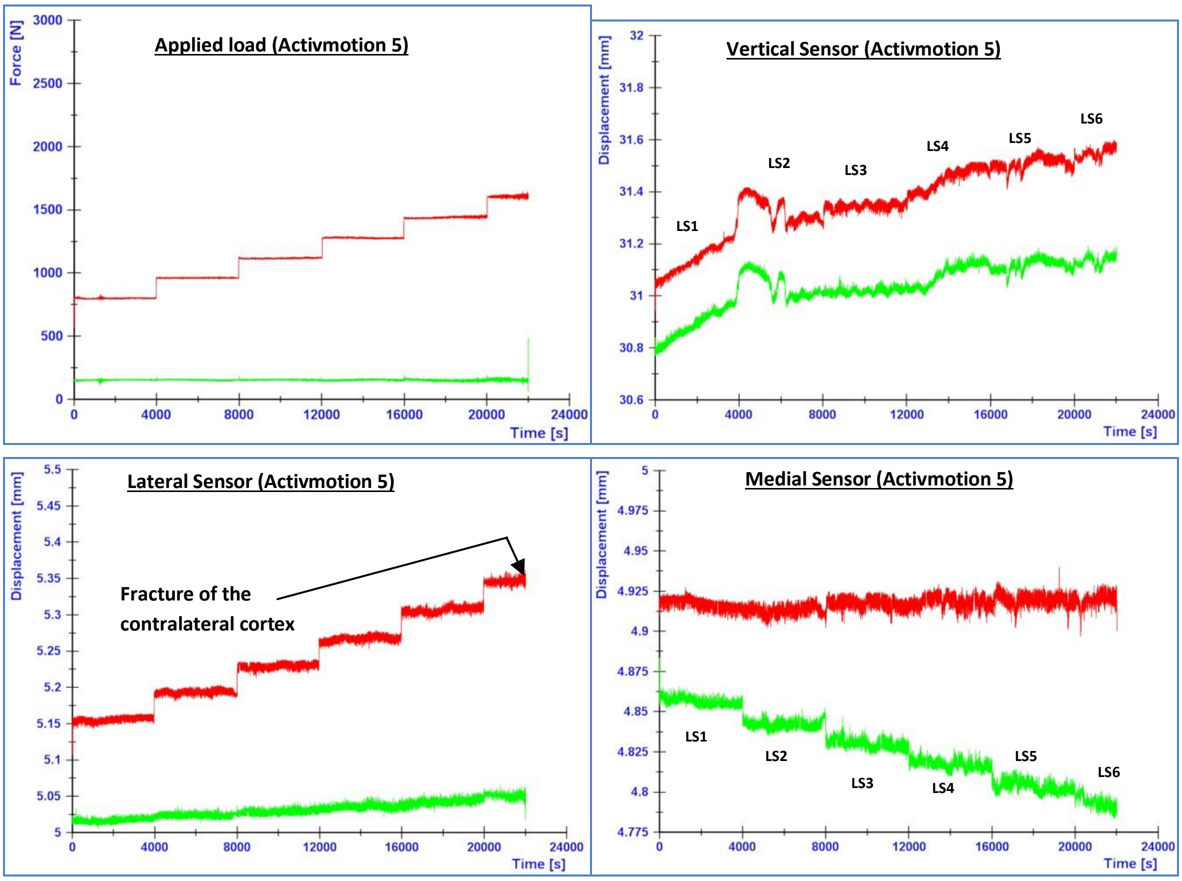

Figure 14: Activmotion 5: Time histories of the applied load, the vertical, the medial and lateral displacements

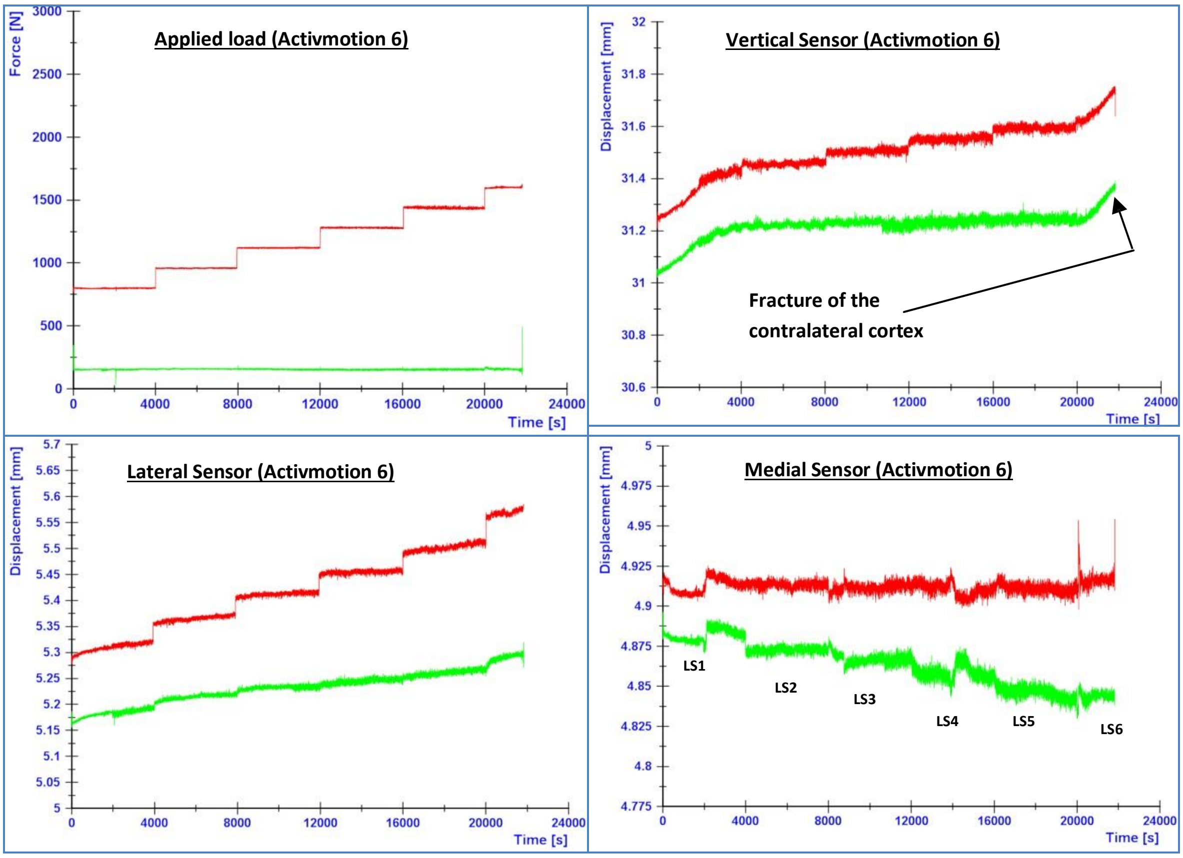

Figure 15: Activmotion 6: Time histories of the applied load, the vertical, the medial and lateral displacements

4.2. Dynamic stiffness

The different "dynamic stiffnesses" of the specimens (vertical, medial and lateral) have been calculated as the ratio of peak to peak force ∆F to the measured peak to peak displacement ∆X in the same period T (**Figure 16**).

$$K = \frac{\Delta F}{\Delta X}$$

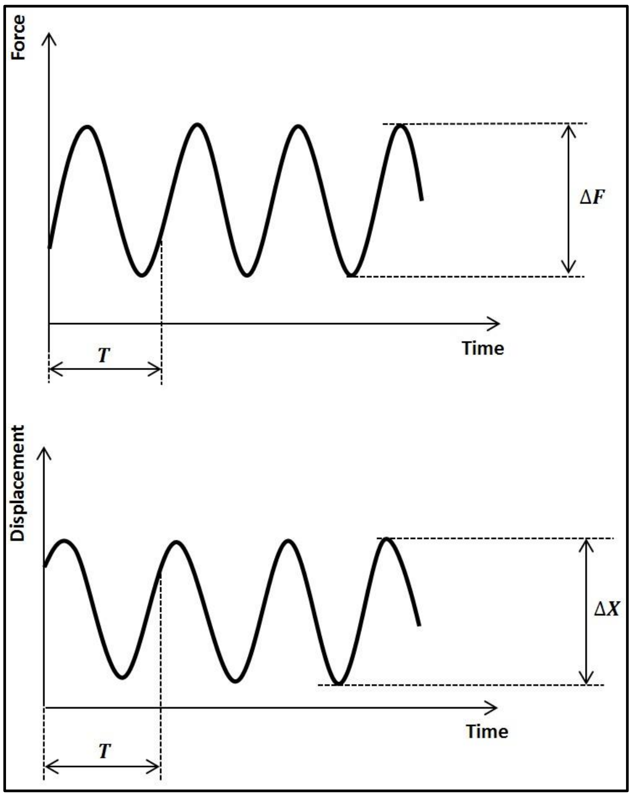

Figure 16: Definition of ΔF and ΔX to calculate the dynamic stiffness for the cyclic fatigue to failure tests

The dynamic stiffness is an additional parameter that could be used to check the failure of the specimen. It normally increases when the specimens is compacting and becoming stiffer under the applied loads, and decreases when damages are occurring in the specimen.

The plots from **Figure 17** to **Figure 20** show the dynamic stiffnesses obtained for the vertical and the lateral displacements for all the specimens that have been subjected to the load controlled fatigue tests. The medial side is not of interest as much as the lateral side, because the failure occurred in the contralateral cortex and the behavior of the medial side is governed by the plate.

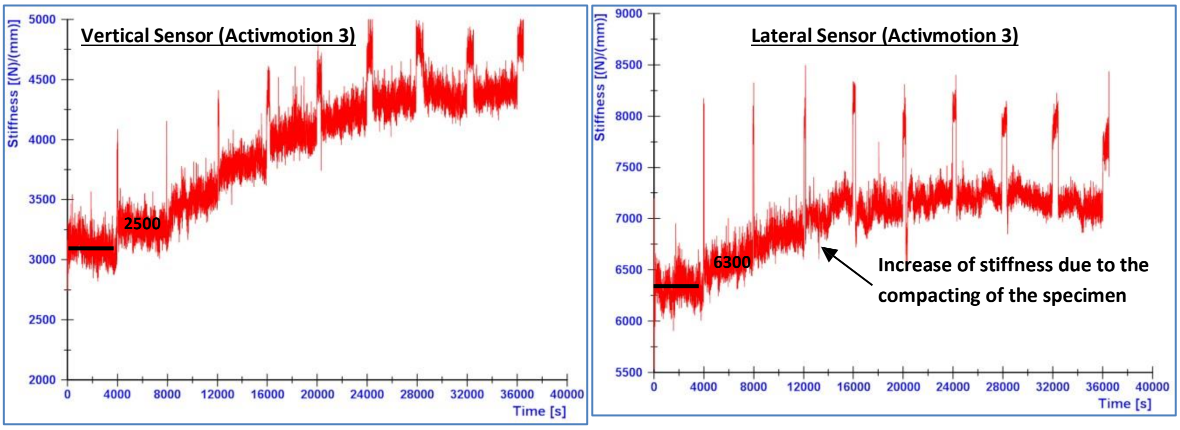

Figure 17: Activmotion 3: Time variation of the stiffnesses during the loading

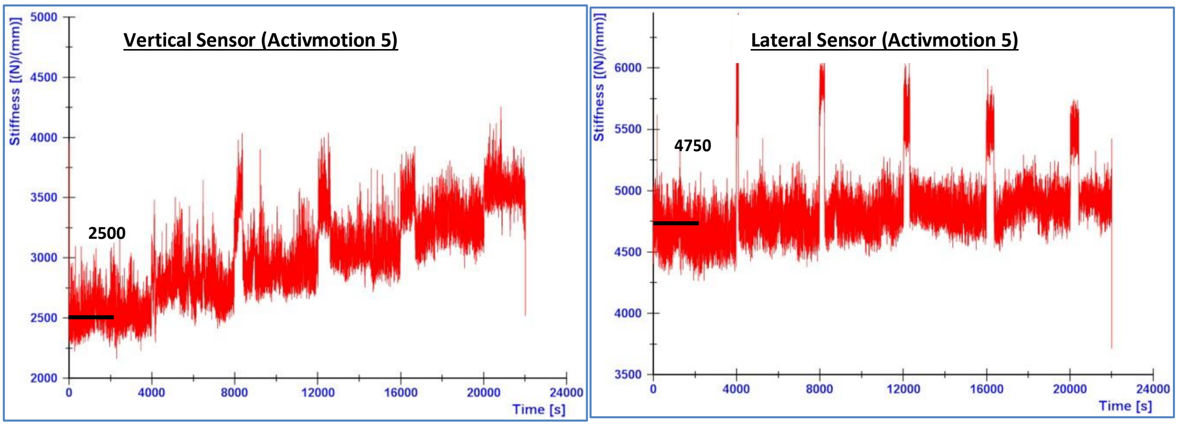

Figure 18: Activmotion 5: Time variation of the stiffnesses during the loading

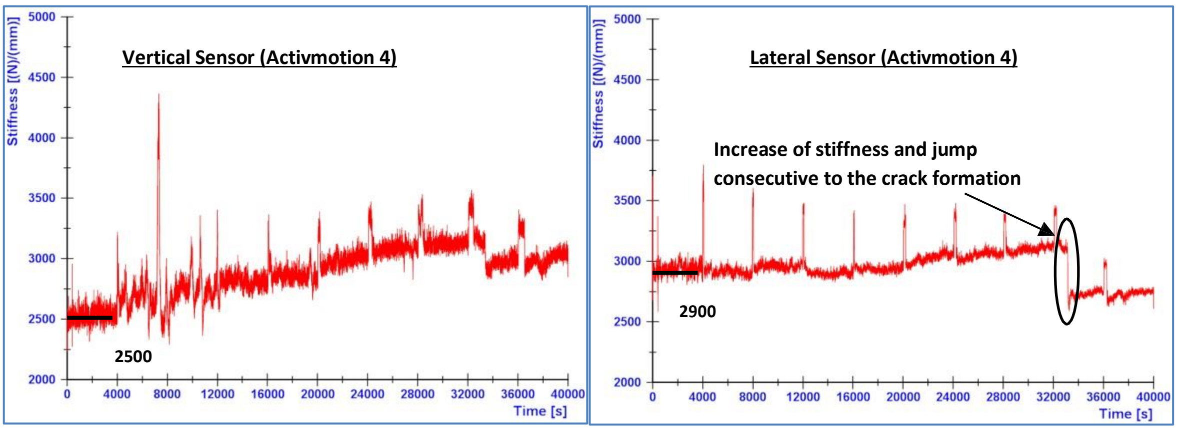

Figure 19: Activmotion 4: Time variation of the stiffnesses during the loading

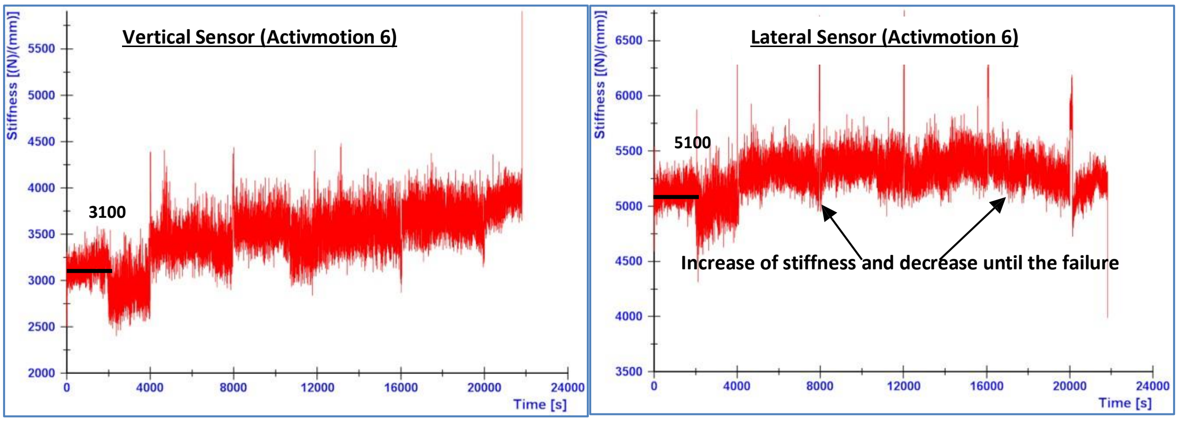

Figure 20: Activmotion 6: Time variation of the stiffnesses during the loading

The values of these different stiffness's, right at the beginning of the first loading step are indicated in **Table 4.**

Specimens	Activmotion 3	Activmotion 4	Activmotion 5	Activmotion 6
Vertical Stiffness (N/mm)	2500	2500	2500	3100
Lateral Stiffness (N/mm)	6300	2900	4750	5100

Table 4: Values of the vertical and lateral stiffnesses of the different specimens subjected to the cyclical tests

4.3. Plastic Deformation and plastic deflection (loss of correction)

The permanent plastic deformation has been estimated here as the irrecoverable displacement from the start of the tests at the minimal force of 160 N, considered as nearly zero force. Hence the permanent plastic deformations could be measured online during the cyclic tests at any time (**Figure 21**), for example before failure (U_{PB}) and additionally after the gross failure, i.e. the collapse of the lateral cortex (U_{PA}) in general (Maas, Diffo Kaze, Dueck, & Pape, 2013; Diffo Kaze, et al., 2015; Diffo Kaze A. , 2016).

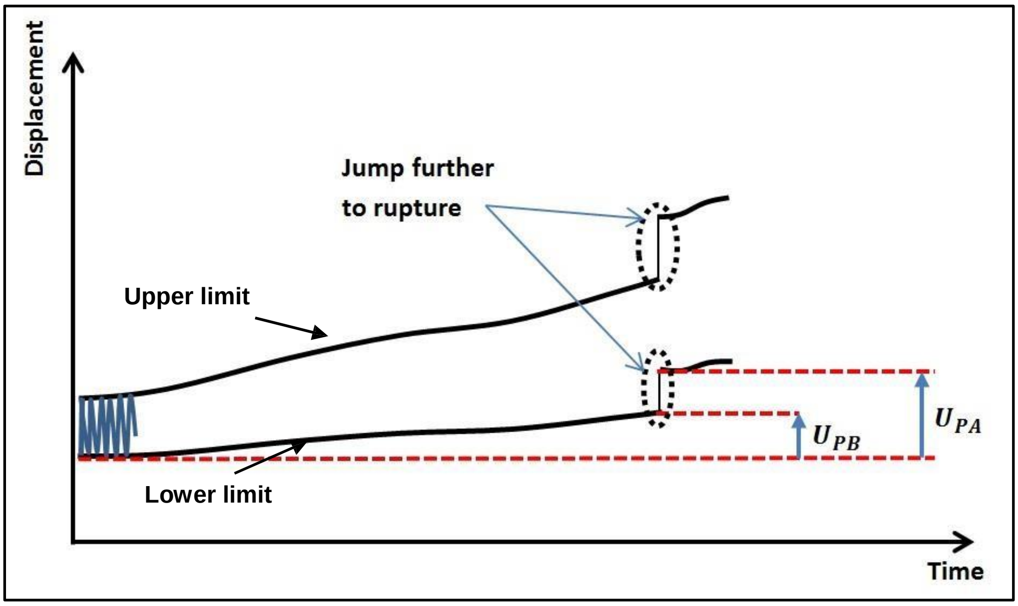

Figure 21: Plastic deformation before and after failure: U_{PB} and U_{PA}

The permanent plastic deflection of the tibia plateau leads to a permanent plastic deflection angle and was calculated as the resulting permanent plastic displacements on the medial and the lateral sides in the specimens' frontal plane, at a given time (**Figure 9**). According to these definitions and the denominations indicated in Figure **9**, the deflection angle (in radians) was defined and could be calculated at any time as

$$\alpha = \frac{d_L - d_M}{D}.$$

According to the definitions of the permanent plastic deformations the failure type 1 occurs when

$$\frac{d}{D} |d_{Lp} - d_{Mp}| > 2 \text{ mm},$$

i.e. if $\alpha_p > 0.024$ rad or 1.4°, with α_p, d_{Lp} and d_{Mp} being the permanent plastic deflection angle, permanent plastic lateral displacement and permanent plastic medial displacement, respectively.

Due to the abrupt fracture of the specimens during the cyclical testing and the fact that the cracking observed in the case of Activmotion 4 has not been considered as a failure, the permanent plastic displacements have been determined only before failure, as indicated in the following pictures (from **Figure 22** to **Figure 25**).

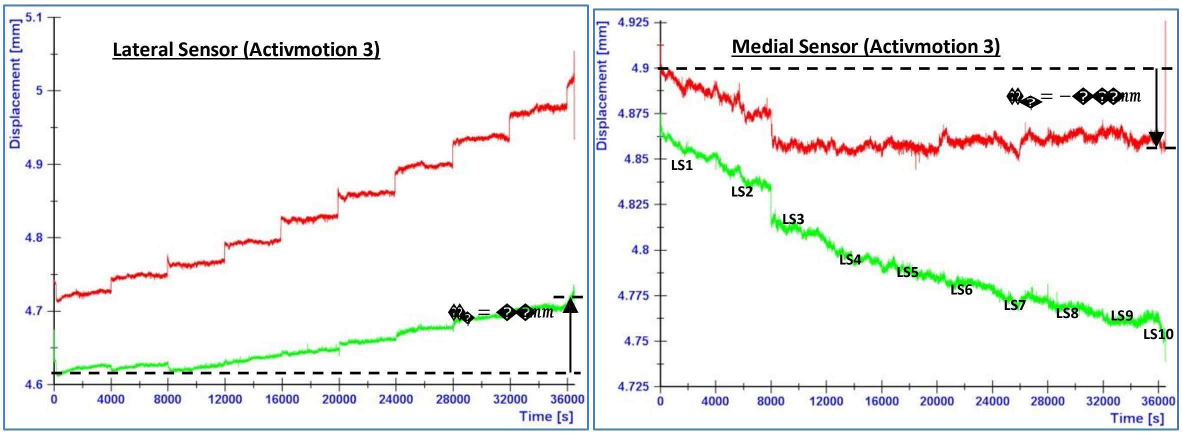

Figure 22: Activmotion 3: Determination of the permanent plastic lateral displacement (d_{Lp}) and medial displacement (d_{Mp}). The medial displacement is counted negatively.

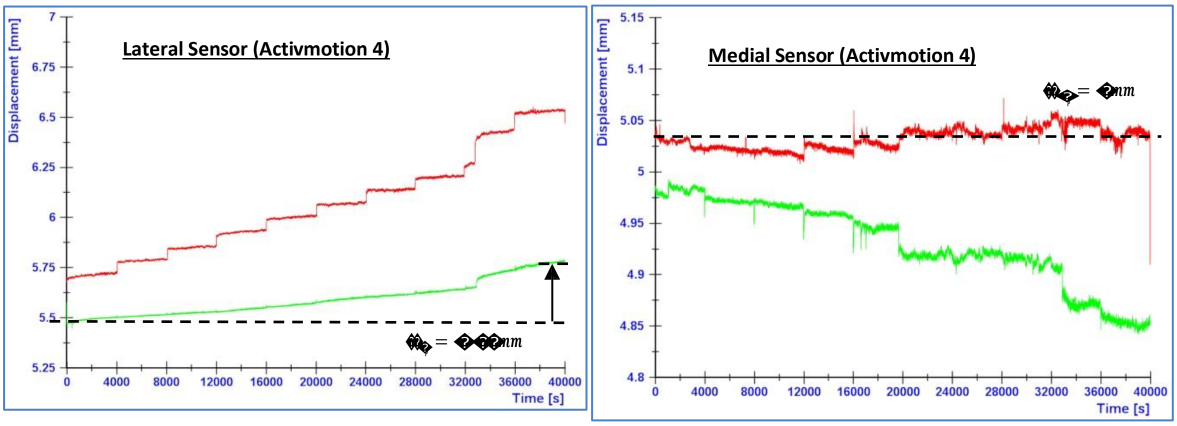

Figure 23: Activmotion 4: Determination of the permanent plastic lateral displacement (d_{Lp}) and medial displacement (d_{Mp})

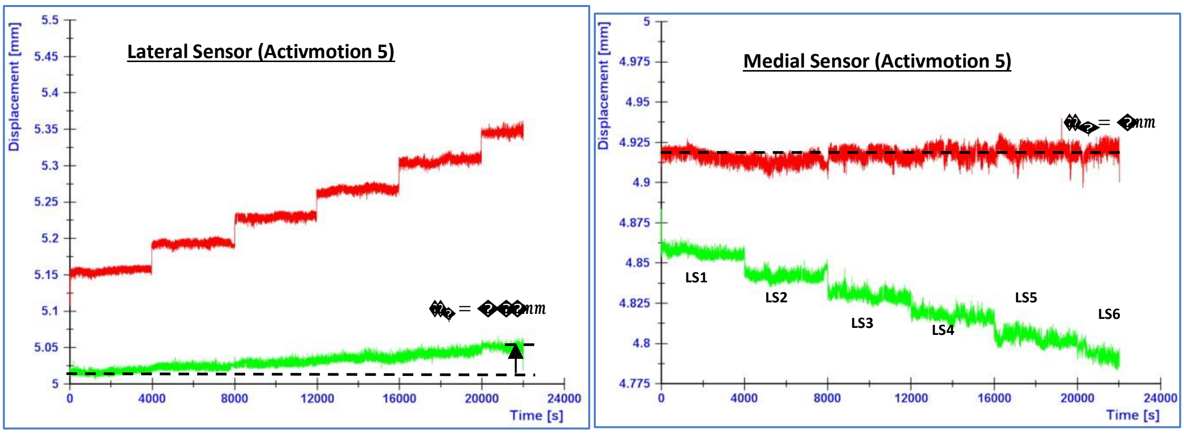

Figure 24: Activmotion 5: Determination of the permanent plastic lateral displacement (d_{Lp}) and medial displacement (d_{Mp})

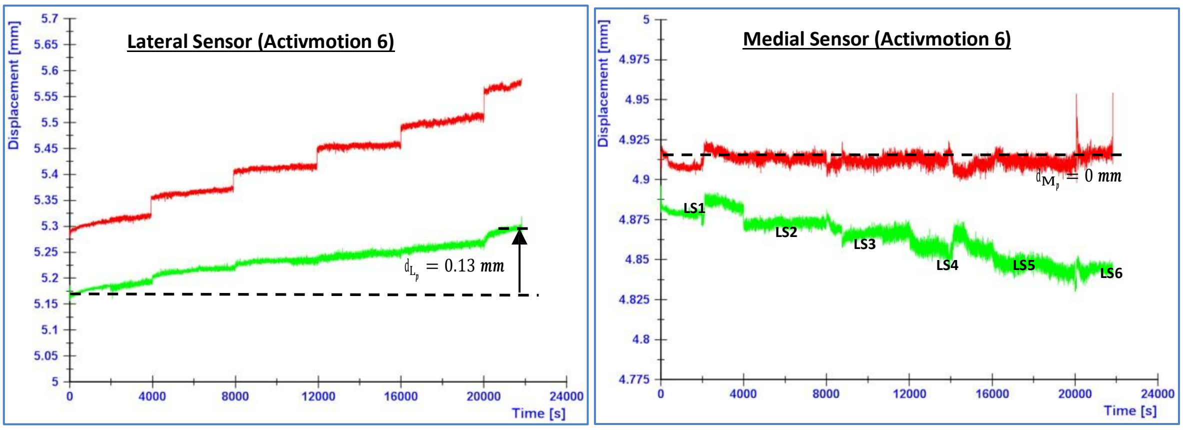

Figure 25: Activmotion 6: Determination of the permanent plastic lateral displacement (d_{Lp}) and medial displacement (d_{Mp})

The **Table 5** gives the medial and lateral permanent plastic displacements, the permanent plastic deflections and the permanent deflection angles before the failure (collapse of the contralateral cortex).

		Activmotion 3	Activmotion 4	Activmotion 5	Activmotion 6
Before failure	Medial (mm)	-0,04	0	0	0
	Lateral (mm)	0,1	0,32	0,03	0,13
	Deflection (mm)	0,14	0,32	0,03	0,13
	Angle (rad)	0.001	0.003	0.0003	0.001
	Angle (Degree)	0,07	0,15	0,014	0,06

Table 5: Plastic deformations of the specimens. Values are rounded to the last decimal

The **Figure 26** recapitulates the permanent deflection angles obtained before the failure. No value is higher than 1,4 degrees; this means that the failure type 1 did not occur for the specimens subjected to the cyclical tests.

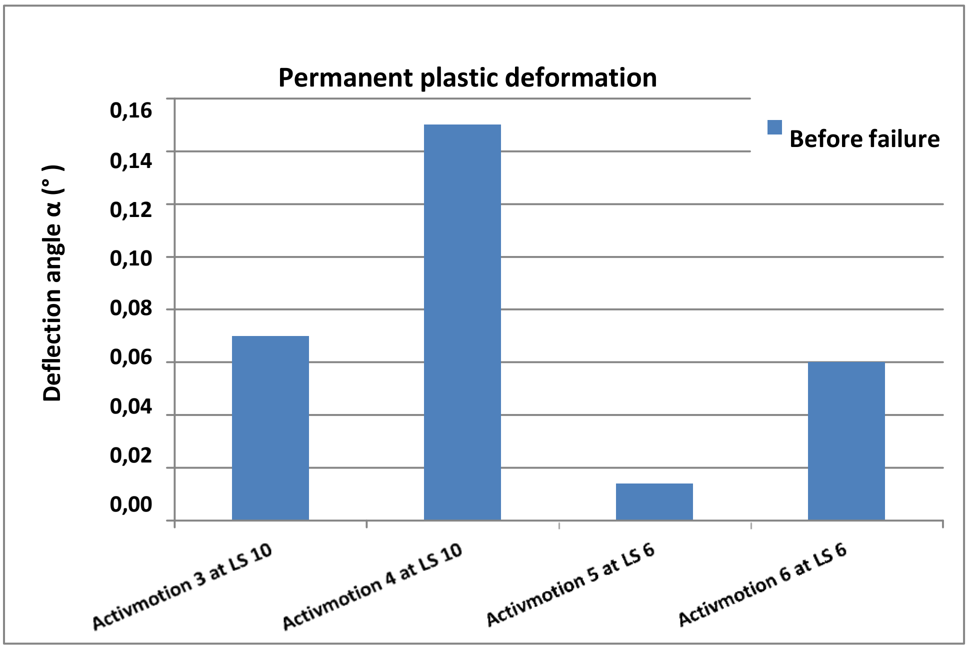

Figure 26: Permanent plastic deflection angle before the failure

4.4. Hysteresis curves: applied force versus displacements

The hysteresis curves are used in order to check the failure type 3 (**Table 2**). This is done by plotting the force versus the displacement. In cases of nonlinear systems, the plot is ideally an elliptical curve with a slope proportional to the stiffness of the system and an enclosed area proportional to the damping of the system, which is being tested. The width of the hysteresis curve represents the maximal displacement range; it increases if the specimen becomes unstable and starts to wobble.

The registered displacements are too noisy, hence the plots of the force versus the displacement are not hysteresis curves in the most cases, as shown for example in the pictures from **Figure 27** to **Figure 29**, except for the lateral displacements of the specimens Activmotion 4 (**Figure 30**) and Activmotion 6 (**Figure 31**), for which it has been possible to determine the maximal width of the hysteresis curve, hence checking failure type 3.

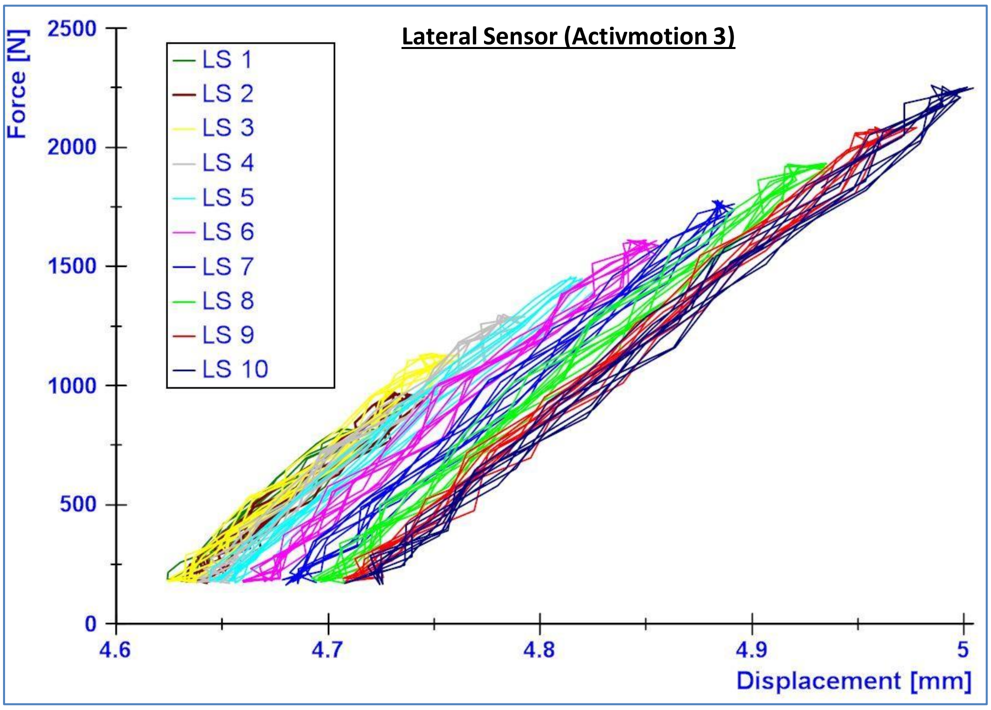

Figure 27: Activmotion 3: Curves force versus lateral displacement

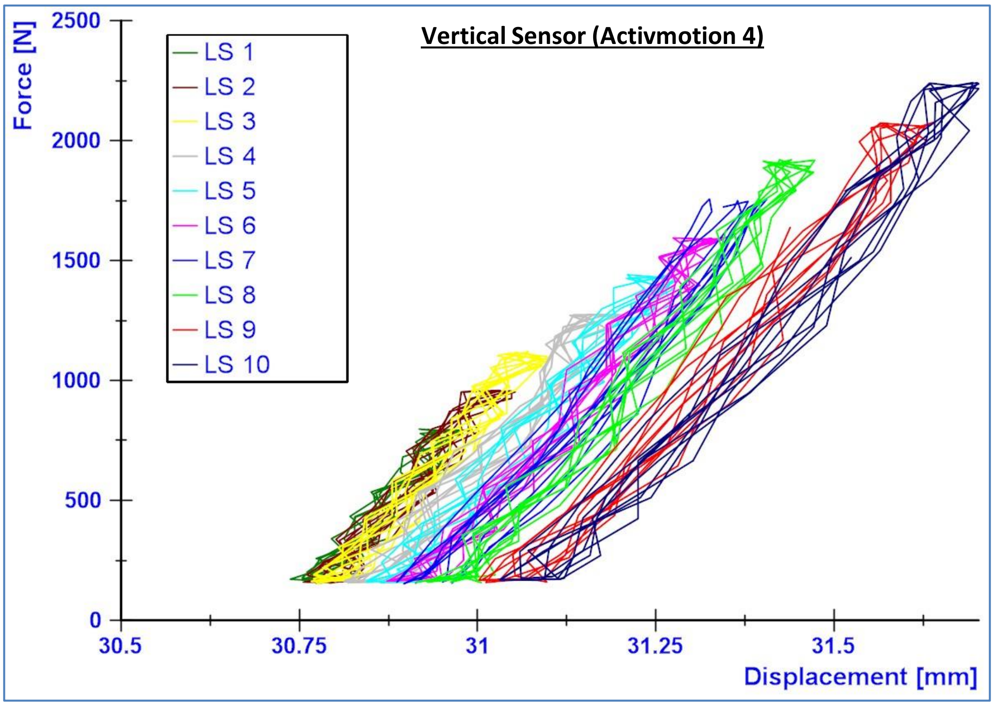

Figure 28: Activmotion 4: Curves force versus vertical displacement

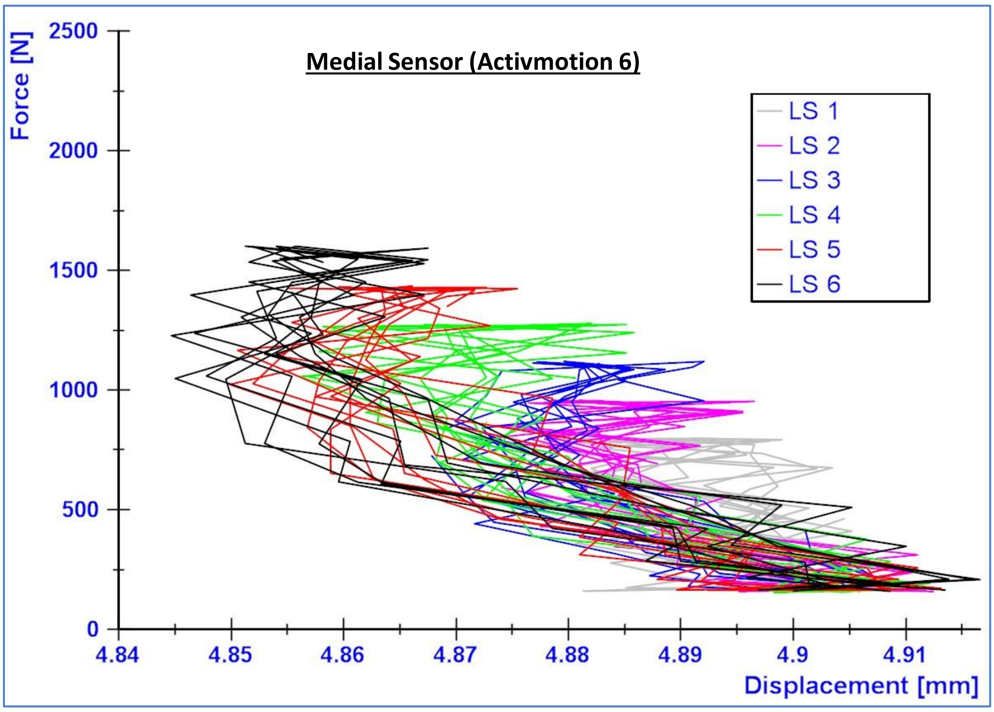

Figure 29: Activmotion 6: Curves force versus medial displacement

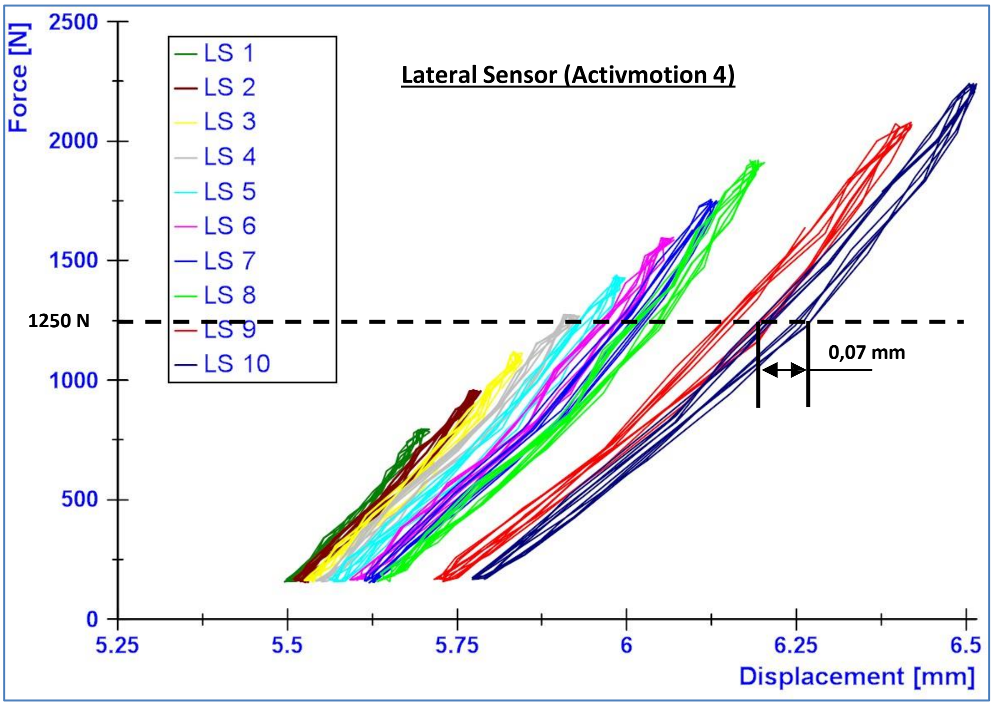

Figure 30: Activmotion 4: Curves force versus lateral displacement. The maximal displacement range is 0,07 mm

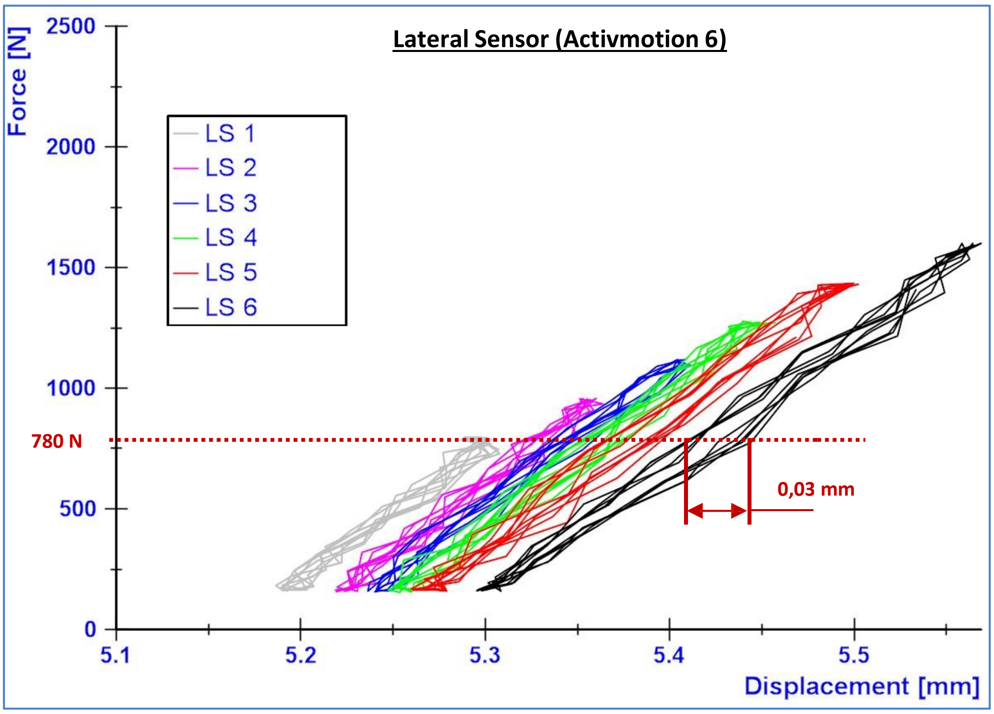

Figure 31: Activmotion 6: Curves force versus lateral displacement. The maximal displacement range is 0,03 mm

The maximal displacement within hysteresis loops, which has been graphically determined (0.03 mm and 0.07 mm) as showed in **Figure 30** and **Figure 31** are all smaller than 0,5 mm. therefore the failure type 3 did not occur for all the specimens tested.

4.5. Summary of the fatigue failure tests

The following **Table 6** gives a summary of the values of the number of cycles of the completely performed load steps, the maximal force before the final fracture of the specimens, and the lateral and the vertical stiffnesses of the specimens at the beginning of the first load step.

Specimen	Load step (LS) / Maximal load [N]	Vertical Stiffness K_V [N/mm]		Lateral Stiffness K_L [N/mm]		Number of cycles	
Activmotion 3	LS10 / 2240	2500	**Mean:2650** **SD±:260**	6300	**Mean:4763** **SD±:1219**	> 180 000	**Mean:> 140 000** **SD±:40 000**
Activmotion 4	LS10 / 2240	2500		2900		> 180 000	
Activmotion 5	LS6 / 1600	2500		4750		> 100 000	
Activmotion 6	LS6 / 1600	3100		5100		> 100 000	

Table 6: Summary of fatigue failure tests (all values before collapse of the specimen): max. load, vertical & lateral stiffness and number of cycles.

5. Comparison with the previous performed tests

Experimental biomechanical studies (Maas, Diffo Kaze, Dueck, & Pape, 2013; Diffo Kaze, et al., 2015) were already performed on other plates (**Figure 2**) using the same materials and methods that have been used to perform the static and the cyclical tests of the present study of the size 2 Activmotion plate (**Figure 1**). Hence the results obtained from all these studies are comparable. The specimens are grouped and subdivided as indicated in **Table 7.**

Performed test	Group 1; n = 5 Specimens	Group 2; n = 5 Specimens	Group 3; n = 6 Specimens	Group 4; n = 5 Specimens	Group 5; n = 5 Specimens	Group 6; n = 6 Specimens
Static: single loading to failure test	TomoFix 1	PEEKPower 1	iBalance 1	TomoFix sm 1	Contour Lock 1	Activmotion 1
	TomoFix 2	PEEKPower 2	iBalance 2	TomoFix sm 2	Contour Lock 2	Activmotion 2
Dynamic: cyclic fatigue failure test	TomoFix 3	PEEKPower 3	iBalance 3	TomoFix sm 3	Contour Lock 3	Activmotion 3
	TomoFix 4	PEEKPower 4	iBalance 4	TomoFix sm 4	Contour Lock 4	Activmotion 4
	TomoFix 5	PEEKPower 5	iBalance 5	TomoFix sm 5	Contour Lock 5	Activmotion 5
			iBalance 6			Activmotion 6

Table 7: Specimen grouping and assignment, depending on used implants and the performed test

5.1. Static loading to failure

The results of the static tests performed on the Activmotion (**Table 3**) are summarized together with the results of the previous studies in **Table 8.** The static lateral stiffness is calculated as the ratio of the applied load to the lateral displacement. The highest average ultimate load, at which the specimens collapsed during the single loading to failure test, is 8.2 kN and obtained for the group 6 (Activmotion). The specimens Contour Lock 1 and 2 showed the largest average lateral displacement (4.1 mm) at fracture of the lateral cortex. The group iBalance showed the highest lateral stiffness at ultimate load (3.1 kN/mm).

The average displacement on the medial compared to the lateral side was always smaller for all implant types. The determined valgus-malrotation of the tibial head was greater or equal to the fixed limit of 1.4° of the permanent deflection angle for all implants, except for the iBalance and Activmotion specimens, which showed the mean values 0.9 ° and 1° respectively. The group TomoFix std showed the maximal valgus-malrotation at collapse time of the contralateral cortex (2.8 °).

The overall observation from the static tests is high strength values with small deformations for the Activmotion plate compared to the other implants.

Specimen	Crack / Ultimate load [kN]	Medial displ. at crack/ ultimate load [mm]	Lateral displ. at crack/ ultimate load [mm]	valgus-malrotation of the tibial head at crack/ ultimate load (°)	Lateral stiffness at crack/ ultimate load [kN/mm]	Failure types
TomoFix std 1	4.1 / 5.4	0.6 / 1.2	3.1 / 5.0	1.8 / 2.9	1.3 /1.1	1 and 2
TomoFix std 2	5.1 / 5.2	1.0 / 1.1	4.2 / 4.4	2.5 / 2.6	1.2 / 1.2	1 and 2
Mean:	**4.6 / 5.3**	**0.8 / 1.2**	**3.7 / 4.7**	**2.1 / 2.8**	**1.3 / 1.1**	
SD ±:	**0.7 / 0.1**	**0.3 / 0.1**	**0.8 / 0.4**	**0.5 / 0.2**	**0.1 / 0.1**	
PEEKPower 1	- / 3.7	- / 0.5	- / 2.9	- / 1.6	- / 1.3	1 and 2
PEEKPower 2	4.2 / 5.1	0.1 / 0.1	2.7 / 3.3	1.3 / 1.5	1.6 / 1.5	1 and 2
Mean:	**- / 4.4**	**- / 0.3**	**- / 3.1**	**- / 1.6**	**- / 1.4**	
SD ±:	**- / 0.1**	**- / 0.3**	**- / 0.3**	**- / 0.1**	**- / 0.1**	
iBalance 1	- / 5.7	- / 0.3	- / 1.6	- / 0.6	- / 3.6	2
iBalance 2	- / 5.4	- / 0.3	- / 2.1	- / 1.1	- / 2.6	2
Mean:	**- / 5.5**	**- / 0.3**	**- / 1.9**	**- / 0.9**	**- / 3.1**	
SD ±:	**- / 0.2**	**- / 0**	**- / 0.4**	**- / 0.4**	**- / 0.7**	
TomoFix sm 1	3.1 / 3.2	0.6 / 0.9	1.3 / 1.8	0.9 / 1.3	2.4 / 1.8	2
TomoFix sm 2	3.2 / 3.6	0.4 / 0.6	1.6 / 2.3	0.9 / 1.4	2.0 / 1.6	2
Mean:	**3.2 / 3.4**	**0.5 / 0.8**	**1.5 / 2.1**	**0.9 / 1.4**	**2.2 / 1.7**	
SD ±:	**0.1 / 0.3**	**0.1 / 0.2**	**0.2 / 0.4**	**0 / 0.1**	**0.3 / 0.1**	
Contour Lock 1	2.4 / 3.2	0.6 / 0.5	2.5 / 3.9	1.5 / 2.1	1.0 / 0.8	1 and 2
Contour Lock 2	- / 3.9	- / 0.5	- / 4.2	- / 2.2	- / 0.9	1 and 2
Mean:	**- / 3.6**	**- / 0.5**	**/ 4.1**	**- / 2.2**	**- / 0.9**	
SD ±:	**- / 0.5**	**- / 0**	**/ 0.2**	**- / 0.1**	**- / 0.1**	
Activmotion 1	- / 8.9	- / 1.3	- / 2.5	- / 0.6	- / 3.6	2
Activmotion 2	3.7 / 7.5	0.7 / 2.1	2.6 / 5.1	0.9 / 1.4	1.4 / 1.5	1 and 2
Mean:	**- / 8.2**	**- / 1.7**	**- / 3.8**	**- / 1.0**	**- / 2.6**	
SD ±:	**- / 0.7**	**- / 0.4**	**- / 1.3**	**- / 0.4**	**- / 1.1**	

Table 8: Static tests summary: Displacements, valgus-malrotation of the tibia head and their corresponding crack and ultimate loads, including mean values and standard deviations (SD). The values of the first 5 groups are retrieved from our previous studies and reported here for purposes of comparison.

5.2. Fatigue loading to failure

The failure type 3, which is checked by means of the maximal displacement range within hysteresis loops, did not occur in the Activmotion group, as well as in the groups 1, 2 and 3. This failure type occurred only in the groups of TomoFix sm and Contour Lock (Maas, Diffo Kaze, Dueck, & Pape, 2013; Diffo Kaze, et al., 2015; Diffo Kaze A. , 2016).

The crack formation observed prior to the collapse of the specimen Activmotion 4 (**Figure 11**) was not considered as failure and the other fractures observed were not preceded with visible cracking. Hence the permanent plastic valgus-malrotation of the tibia before and after the failure was considered to be the same for the group Activmotion. The values of the permanent plastic valgus-malrotation are summarized in **Figure 32** for the groups 1, 2, 3 and 6. **Figure 33** shows the permanent plastic deflection angle in the groups 4 and 5. The load history according to **Figure 3** is indicated with the Load Step number (LSn) at which the failure occurred. The failure type 1, which is characterized by a permanent plastic deflection angle greater than 1.4 °, occurred only in the groups of the iBalance, TomoFix sm and Contour Lock.

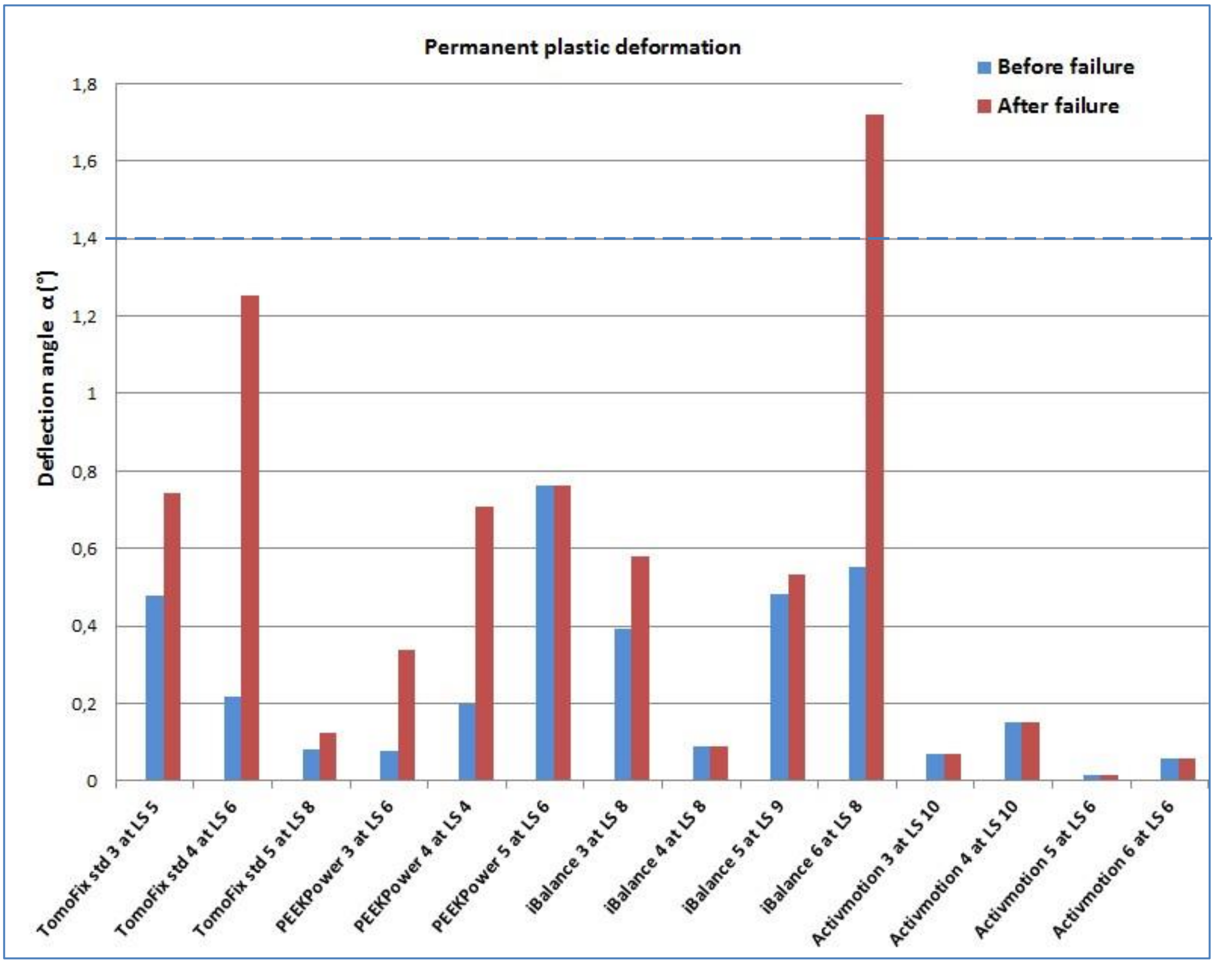

Figure 32: Deflection angle or valgus-malrotation of the tibia head before and after the failure for groups 1, 2, 3 and 6. The failure type 1 was observed in the case of the specimen iBalance 6 after the collapse of the opposite cortex. LS "n" means the failure occurred at load step "n". The values of the first 3 groups are retrieved from our previous studies.

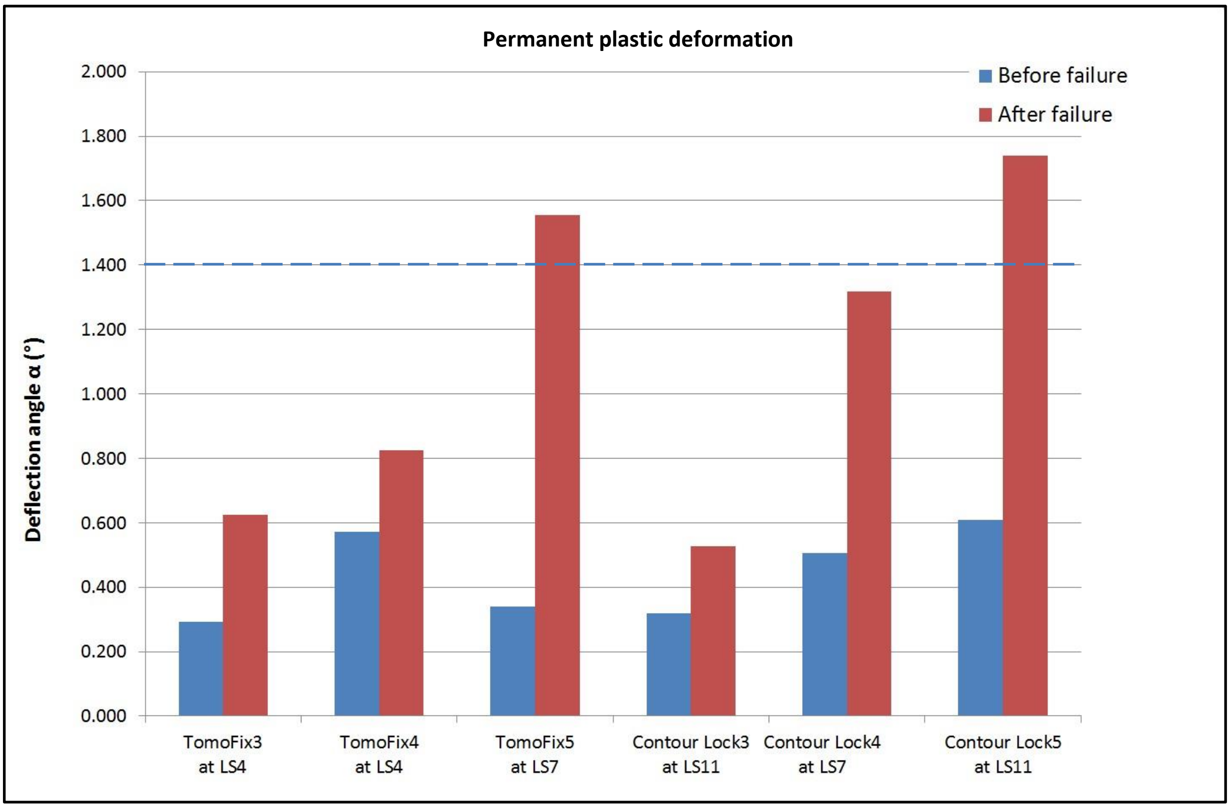

Figure 33: Deflection angle or valgus-malrotation of the tibia head before and after the failure for groups 4 and 5 (From our previous studies). The TomoFix specimens here are the TomoFix small stature of the group 4 of the present study. The failure type 1 was thus observed for the specimens TomoFix sm 5 and Contour Lock 5.

For sake of comparison, the results of fatigue loading to failure from our previous studies are presented here, together with the results obtained from the testing on the Activmotion plate, in the **Table 9, Table 10**, which summarize the results of the cyclic fatigue to failure tests by listing the maximal compressive force, lateral and the vertical stiffness of the specimens at the beginning of the first load step, the number of cycles performed prior to the failure and the types of failure.

Specimen	Maximal load [N]	Vertical stiffness K_V [N/mm]	Lateral stiffness K_L [N/mm]	Number of cycles	Failure types
TomoFix std 3	1280	1350	2000	> 60 000	2
TomoFix std 4	1440	2000	2500	> 80 000	2
TomoFix std 5	1760	2500	2200	> 120 000	2
PEEKPower 3	1440	2000	2500	> 80 000	2
PEEKPower 4	1280	1950	2140	> 60 000	2
PEEKPower 5	1440	2785	2250	> 80 000	2
iBalance 3	1760	4000	3600	> 120 000	2,4
iBalance 4	1760	3000	3400	> 120 000	2
iBalance 5	1920	3000	2952	> 140 000	2
iBalance 6	1760	3500	2500	> 120 000	1,2

Table 9: Summary of fatigue failure tests (Groups 1, 2 & 3): max. load, vertical & lateral stiffnesses, number of cycles (all values prior to failure) and failure types.

Specimen	Maximal load [N]	Vertical Stiffness K_V [N/mm]	Lateral Stiffness K_L [N/mm]	Number of cycles	Failure type
TomoFix sm 3	1280	2200	2000	> 60 000	2,3
TomoFix sm 4	1280	1750	1500	> 60 000	2,3
TomoFix sm 5	1760	2000	2300	> 120 000	1,2
Contour Lock 3	2400	2100	4400	> 200 000	2
Contour Lock 4	1760	2300	2400	> 120 000	2
Contour Lock 5	2400	2700	2600	> 200 000	1,2,3
Activmotion 3	2240	2500	6300	> 180 000	2
Activmotion 4	2240	2500	2900	> 180 000	2
Activmotion 5	1600	2500	4750	> 100 000	2
Activmotion 6	1600	3100	5100	> 100 000	2

Table 10: Summary of fatigue to failure tests (Groups 4, 5 & 6): max. load, vertical & lateral stiffnesses, number of cycles (all values prior to failure) and failure types. The values of the group 4 and 5 are retrieved from our previous studies and reported here for sake of comparison

For the group 6 only the failure type 2, i.e., collapse of the contralateral cortex was observed (**Table 10**). A damage of the fixation system, i.e, failure type 4 occurred in the iBalance group.

Table 11 shows mean values per group of the characteristic values given in the **Table 9** and **Table 10** of the individual specimens.

Groups	Maximal load [kN]		Vertical stiffness K_V [N/mm]		Lateral stiffness K_L [N/mm]		Number of cycles prior to failure	
	Mean	SD ±	Mean	SD ±	Mean	SD ±	Mean	SD ±
TomoFix std	1.5	0.2	1950	577	2233	252	> 86 000	30 550
PEEKPower	1.4	0.1	2245	468	2297	184	> 73 000	11 500
iBalance	1.8	0.1	3375	479	3113	490	> 125 000	10 000
TomoFix sm	1.4	0.3	1983	184	1933	330	> 80 000	28 300
Contour Lock	2.2	0.4	2367	250	3133	900	> 173 000	37 700
Activmotion	1.9	0.3	2650	260	4763	1219	> 140 000	40 000

Table 11: Average mean values, including the standard deviations (SD), per group of the cyclic fatigue to failure tests (All comma values rounded to the 1st decimal). The values of the first 5 groups are retrieved from our previous studies and reported here for purposes of comparison.

Regarding the parameters investigated for the fatigue loading to failure tests the Contour Lock group showed the highest values followed by the Activmotion. The highest lateral and medial stiffness was showed by the Activmotion and the iBalance group respectively. PEEKPower group showed higher stiffnesses compared with the TomoFix plates.

Figure 34 shows the average relative values per groups of the cyclic tests that have been calculated based on **Table 11** and by taking the group TomoFix std as reference.

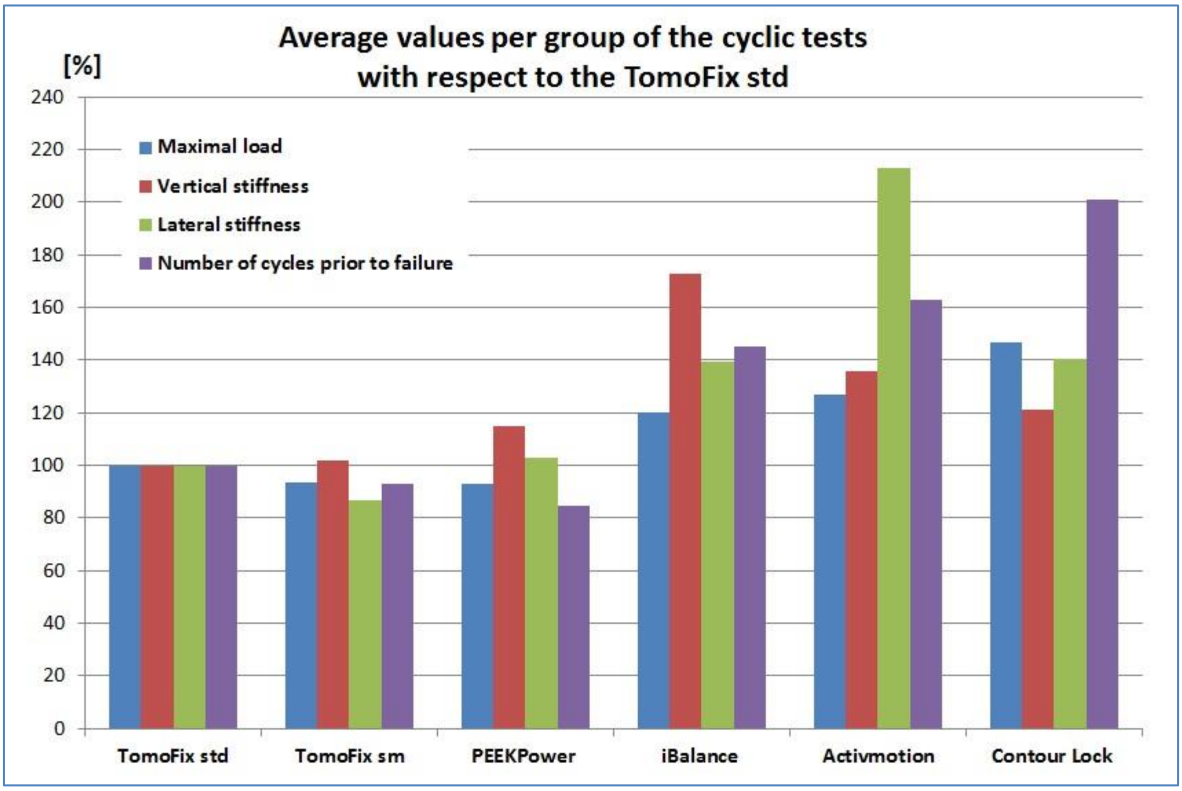

Figure 34: Average relative strength values of Table 6. The TomoFix std group has been taken as reference

The life span of the Contour Lock specimens prior to failure was in average twice as long as for the TomoFix std specimens. The vertical stiffness of the iBalance group was in average around 1.7 higher than the one of the TomoFix std group. The lateral stiffness of the Activmotion group is more than twice the one of the the TomoFix std group.

6. Conclusion

In this study the Activmotion plate was investigated and compared to our previous studies using the same experimental setup and protocol, thus comparing the static and fatigue fixation stability provided by the Activmotion plate to the one provided by the following five different medial open wedge HTO-plates: The TomoFix std plate, the PEEKPower plate, the iBalance implant, the Contour Lock HTO plate and the TomoFix sm plate. The key findings of the present study were that: (1) the stiffest bone-implant construct was found to be the Activmotion plate followed by the Contour Lock plate. (2) The Contour Lock plate provided the highest fatigue strength under cyclic loading conditions. (3) Static loading until failure tests revealed superior strength of the Activmotion plate followed by the ibalance implant, the TomoFix std, the PEEKPower plate, the Contour Lock and the TomoFix sm plates. (4) All implants withstood the maximal physiological vertical tibiofemoral contact force while slow walking. This force is about 3 times the body weight (Heinlein et al. 2009; Taylor et al. 2004), e.g. 2400 N for a patient weighing 80 kg.

All the tested bone-implant-constructs failed eventually due to the collapse of the opposite cortex, regardless whether a static or cyclic failure test was applied, as for the cases of our previous study. The final fracture of the contralateral cortex was not generally preceded by a cracking as it was usually the case in previous studies, except for the specimen Activmotion 4. The displacements of the lateral side of the osteotomy were more pronounced than the medial displacement, which explains the valgus rotation in the frontal plane of the tibial head during the static and the cyclic loading tests.

During the static loading to failure test, the average ultimate force of the Activmotion was 8.2 kN, a value which is higher compared to the average values from our previous studies, namely 5.3 kN, 4.4 kN, 3.6 kN and 3.4 kN for the iBalance, the TomoFix std, the PEEKPower, the Contour Lock and the TomoFix sm group respectively. Hence, the Activmotion is superior regarding the static performance.

The maximal load at failure that were observed during the fatigue tests for the Activmotion group was in average 1,9 kN. Considering the number of cycles and the maximal load at failure, the Contour Lock plate showed the best performance with 2.2 kN and 173000 cycles, followed by the Activmotion plates with 1.9 kN and 140000 cycles. Based on those two parameters a ranking for the cyclic tests would place the iBalance in the third position after the Activmotion (2^{nd}) and the Contour Lock plate (1st), then the TomoFix std (4^{th}) followed by the TomoFix sm (5^{th}) and the PEEKpower (6^{th}).

A valgus deformation of the knee will result from the valgus-malrotation of the tibial head, which occurred during the tests, and consequently alter the localisation of the mechanical axis and the primary performed correction. No permanent plastic valgus-malrotation of the tibial head, which led to failure type 1, was observed in the Activmotion group. Permanent plastic valgus-malrotations resulting in failure type 1 before fracture of the contralateral cortex were in the groups of the iBalance, the TomoFix sm and of the Contour Lock, as shown in **Figure 32** and **Figure 33**. Hence, it can be assume that the TomoFix std and the PEEKPower plates better conserve correction compare to the iBalance, Tomofix sm and Contour Lock implants, but the Activmotion provides the best results of all due to its relative higher number of performed loading cycles before failure. It is cautioned at this level that the last observation is only valid if there is no bone healing prior to the fatigue failure, which is not a realistic scenario.

7. References

1. Diffo Kaze, A. (2016). *Etude biomécanique comparative de cinq différents systèmes de fixation utilisés dans les cas d'ostéotomies tibiales valgisantes: Essais expérimentaux et simulations numériques incluant les forces musculaires.* University of Luxembourg. Aachen: SHAKER VERLAG.

2. Diffo Kaze, A., Maas, S., Waldmann, D., Zilian, A., Dueck, K., & Pape, D. (2015). Biomechanical properties of five different currently used implants for open-wedge high tibial osteotomy. *Journal of Experimental Orthopaedics, 2*(14). doi:10.1186/s40634-015-0030-4

3. ISO 7206-4. (1989). Implants for surgery: Determination of endurance properties of stemmed femoral components with application of torsion.

4. ISO 7206-6. (1992). Implants for surgery: Determination of endurance properties of head and neck region of stemmed femoral components.

5. ISO 7206-8. (1995). Implants for surgery: Endurance performance of stemmed femoral components with application of torsion.

6. Maas, S., Diffo Kaze, A., Dueck, K., & Pape, D. (2013). Static and Dynamic Differences in Fixation Stability between a Spacer Plate and a Small Stature Plate Fixator Used for High Tibial Osteotomies: A Biomechanical Bone Composite Study. *ISRN Orthopedics, 2013*. doi:10.1155/2013/387620

7. Pape, D.; Lorbach, O.; Schmitz, C.; Busch, L. C.; Van Giffen, N.; Seil, R.; Kohn, D. M. (2010). Effect of a biplanar osteotomy on primary stability following high tibial osteotomy: a biomechanical cadaver study. *Knee Surg Sports Traumatol Arthrosc., 18*, 204-211.